$E1$ and $E2$-$E0$ Form Factors and Strength Distributions from ^{28}Si$(e,e'p)$ and ^{28}Si$(e,e'\alpha)$ Coincidence Scattering

Th. Kihm, K. T. Knöpfle, H. Riedesel, and P. Voruganti
Max-Planck-Institut für Kernphysik, D-6900 Heidelberg, Germany

and

H. J. Emrich, G. Fricke, R. Neuhausen, and R. K. M. Schneider
Institut für Kernphysik, Universität Mainz, D-6500 Mainz, Germany
(Received 19 May 1986)

A model-independent multipole analysis of ^{28}Si$(e,e'p)$ and ^{28}Si$(e,e'\alpha)$ coincidence data, taken at three momentum transfers $0.39 < q < 0.68$ fm^{-1}, yields both $E1$ and $E2$-$E0$ form factors and the respective multipole strength distributions in the giant-resonance region of ^{28}Si ($E_x = 14$–22 MeV). While the deduced $E1$ strength agrees well with previous results, the total extracted $E2$-$E0$ strength is about twice the value found with isoscalar projectiles indicating the presence of large isovector $E2$-$E0$ contributions in the region of the isoscalar $E2$-$E0$ giant resonances.

PACS numbers: 24.30.Cz, 23.20.Js, 25.30.Dh, 27.30.+t

In the nuclear continuum region, the well-established[1,2] inherent power of the (e,e') reaction to map out the Fourier transforms of the transition charge and current densities is in practice seriously impaired by the presence of the large radiative-tail background, which often even surmounts the inelastic excitation, while its precise determination represents a challenging problem by itself.[3] Fortunately, however, the largest part of the radiative tail is due to elastic scattering, and so it will be removed—as the tails of all other bound states—by the detection in coincidence of the inelastically scattered electron and the nuclear decay product c. Such experiments have only recently become feasible by the advent of cw electron accelerators. The present work takes full advantage of the background-free preparation of the nuclear response in $(e,e'c)$ coincidence scattering and develops a novel and, in principle, model-independent multipole analysis of the 4π-integrated $(e,e'c)$ spectra applicable to all measured decay channels, i.e., in particular those where the analysis of angular correlation functions is becoming ambiguous as a result of either complex spin couplings or unresolved final states. We have chosen as target nucleus ^{28}Si because its giant-resonance (GR) region has been studied in detail with various probes. Comparison with the results of photonuclear[4–6] studies allows scrutinization of our results obtained for the giant dipole resonance (GDR), while the comparison with the results of the isospin-selective (α,α')[7–10] and $(\alpha,\alpha'c)$[11] reactions sheds new light on the isospin structure of giant quadrupole (GQR) and monopole (GMR) resonance excitations.

The 183.5-MeV cw electron beam of the Mainz microtron[12] MAMI A at ~ 15-μA current was used to bombard a natural Si target (92% ^{28}Si) of 2.89 mg/cm^2 thickness. Scattered electrons were measured at 25°, 30°, and 45° by the Mainz 180° magnetic spectrometer[13]; the corresponding momentum transfers of $q = 0.39$, 0.47, and 0.68 fm^{-1} cover the maximum of the $E1$ and the increasing slope of the $E0$-$E2$ form factors. Secondary charged-particle decay products $c = p, \alpha$ were detected in coincidence by eight ΔE-E surface-barrier detector telescopes (70 μm, 700 μm, ~ 20 msr) providing a unique particle identification for energies $E_c > 2.5$ MeV. The telescopes were mounted in a plane rotated by $\phi_c = 45°$ around the q axis from the (e,e') scattering plane. The measured angular correlation functions (ACF's) cover the complete angular range $-10° \leq \theta_c \leq 215°$ relative to the q axis in steps of $\sim 10°$. Since (e,e') scattering at forward angles suppresses transverse excitations, the ACF's exhibit to good approximation axial symmetry about the q axis.[14] For each decay channel c, integration of the measured inplane ACF thus leads to the 4π-integrated $(e,e'c)$ coincidence cross section representing the longitudinal nuclear response function in channel c unaffected by any elastic radiative-tail background.

Figure 1 shows a singles ^{28}Si(e,e') spectrum (top) taken at 30° with a resolution of $\simeq 120$ keV. The range of excitation energies E_x—denoted also ω—extends from the charged-particle threshold at ~ 10 MeV up to the region of the GDR and GQR, $16 < \omega < 22$ MeV. At this momentum transfer $E1$ and $E2$-$E0$ GR's are expected to exhibit similar cross sections. The lower part of Fig. 1 shows the 4π-integrated $(e,e'c)$ coincidence cross section in the total charged $c = p, \alpha$ channel. The coincidence requirement has effectively removed the huge elastic radiative tail, so that the transition from isolated resonances to the GR region with its characteristic fine structure becomes clearly visible. Subtracting the 4π-integrated

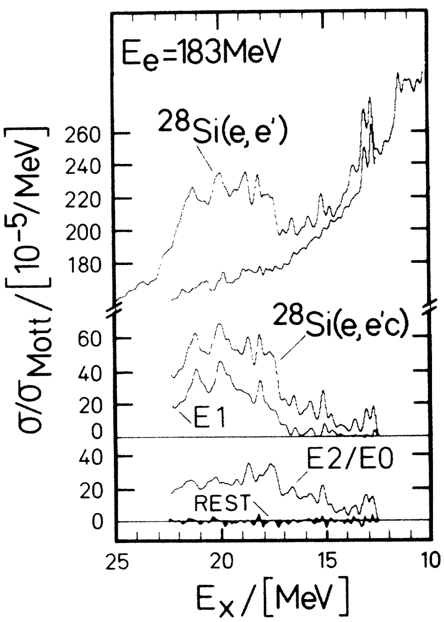

FIG. 1. Upper part: singles (e,e') spectrum at $\theta_{e'} = 30°$ in the GR region of ^{28}Si and its deduced radiative tail (see text). Lower part: 4π-integrated $^{28}\mathrm{Si}(e,e'c)$ coincidence cross section in all $c=p,\alpha$ decay channels and its decomposition into the $E1$ and $E2$-$E0$ components. "Rest" denotes the difference spectrum between measured $(e,e'c)$ yield and the sum of deduced $E1$ and $E2$-$E0$ cross sections.

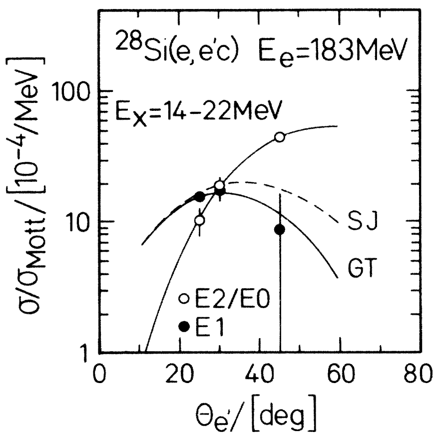

FIG. 2. The deduced $E1$ and $E2$-$E0$ form factors (circles) compared with $E1$ and $E2$ DWBA predictions (curves); the $E1$ transition density is taken from both the Goldhaber-Teller (GT) and Steinwedel-Jensen (SJ) models with $c=1.1c_0$, and the $E2$ transition density from the Tassie model with $c=0.9c_0$.

$(e,e'p)$ and $(e,e'\alpha)$ coincidence cross sections from the singles spectrum yields the difference spectrum (curve below the singles spectrum) which represents up to the neutron threshold at 17.2 MeV the elastic radiative tail; the less rapid falloff above 17.2 MeV indicates the undetected contribution from the neutron channel. The fluctuations of this curve from a smooth flow amount for $13.5 < \omega < 17.2$ MeV to less than 5% of the $(e,e'c)$ yield, verifying experimentally the assumed axial asymmetry of the ACF's about the q axis within the theoretical estimate. (For $\omega < 13.5$ MeV, part of the emitted α particles is stopped in the target causing the peak structures at $\omega \sim 13.5$ MeV.)

Our present approach[15] to a multipole decomposition of the measured nuclear response functions is exclusively based on measured quantities, i.e., the 4π-integrated $(e,e'c)$ coincidence cross sections, $\sigma(q_k,\omega_j)$, discussed above. For each decay channel c, the experimental input consists of 750 data points $|F(q_k,\omega_j)|^2 \equiv \sigma_{\mathrm{expt}}(q_k,\omega_j)/\sigma_{\mathrm{Mott}}$ measured at three momentum transfers q_k $(k=1\text{-}3)$ in the range $12 \le \omega \le 22$ MeV in 250 energy bins ω_j $(j=1\text{-}250)$ of 40-keV width. According to the traditional multipole-expansion method,[16] the measured form factors $|F(q_k,\omega_j)|^2$ are expressed as the linear combination of the different contributing longitudinal multipole components:

$$|F(q_k,\omega_j)|^2 = a_{E1}(\omega_j)|F_{E1}(q_k)|^2 + a_{E2\text{-}E0}(\omega_j)|F_{E2\text{-}E0}(q_k)|^2.$$

This *Ansatz* assumes (i) that only $E0$, $E1$, and $E2$ excitations contribute and (ii) that $E2$ and $E0$ form factors are identical. Traditionally,[15] the multipole coefficients $a_{E\lambda}(\omega_j)$ are determined in each energy bin ω_j by a least-squares fit assuming a q dependence for the form factors $|F_{E\lambda}(q_k)|^2$ as given by a nuclear-model calculation. In order to avoid the well-known[17] problem of the large model dependence of, in particular, the $E1$ form factor, a third assumption is introduced, namely (iii) that between $\omega = 12$ and 22 MeV states of identical multipolarity exhibit identical form factors. Assumption (iii) leads so from $I=250$ independent systems of three linear equations for each energy bin ω_j to a single system of $3I=750$ nonlinear equations with $2I+4=504$ unknown quantities $a_{E1}(\omega_j)$, $a_{E2\text{-}E0}(\omega_j)$ $(j=1\text{-}250)$, and $|F_{E1}(q_k)|^2$, $|F_{E2\text{-}E0}(q_k)|^2$ $(k=2,3)$, which is overdetermined for $I>4$ and solved by a least-squares fit procedure $[|F_{E\lambda}(q_1)|^2$ can be normalized to 1]. Any failure of assumptions (i)–(iii) in any energy bin ω_j will be revealed with extreme sensitivity by a corresponding failure of the fit to reproduce the measured data points of the respective energy bin ω_j.

The deduced integral $E1$ and $E2$-$E0$ form factors are shown in Fig. 2. Within the error bars they agree with the respective $E1$ and $E2$ predictions of the Goldhaber-Teller[18] (GT) and Tassie[19] models in the distorted-wave Born approximation (DWBA) after adjustment[20] of the half-density radius c. The $E1$ fit yielded $c = 1.1c_0$, a model-dependent value leading in the Steinwedel-Jensen[21] model to a significantly worse description of the data (dashed line in Fig. 2). The $E2$ calculation required a value of $c = 0.9c_0$ indicating similar transition radii of GQR and low-lying collective 2^+ states. With use of the GT prediction for the extrapolation to the photon point, the $E1$ strength is found to exhaust $(41 \pm 3)\%$ of the energy-weighted sum rule (EWSR) in the range $14 < \omega < 22$ MeV. This value is compatible with the results from photonuclear studies[4,5] where the difference $\sigma(\gamma,\text{abs}) - \sigma(\gamma,n)$ amounts to $43\% - 8\% = 35\%$ of the EWSR.

The indicated two lower curves in Fig. 1 show the respective $E1$ and $E2$-$E0$ components of the total $(e,e'c)$ yields as determined in the fit procedure. The "rest" spectrum at the bottom represents the difference between the measured cross section and the sum of the extracted $E1$ and $E2$-$E0$ contributions; the corresponding error bands obtained at $\theta_{e'} = 25°$ and $45°$ are similar in size. These error bands—being small —exhibit in general for a given energy bin no correlated deviations at the three different momentum transfers. This establishes the validity of our assumption (iii) that the $E1$ and $E2$-$E0$ form factors are largely independent of excitation energy. If $E2$ and $E0$ strengths are uncorrelated, the agreement between data and fit also implies that the $E2$ and $E0$ form factors agree within the errors shown in Fig. 2.

The present multipole decomposition method is corroborated by comparison of the present $E1$ strength distributions with the respective results from a $^{28}\text{Si}(\gamma,c)$ photodisintegration study[6] with tagged photons. The (γ,c) data were converted to a $(e,e'c)$ cross section by use of an identical normalization for all decay channels c; the absolute $E1$ strengths of both studies are found to agree within the 20% error of the (γ,c) study. Figure 3 reveals nice agreement between the $(e,e'c)$ results and the (γ,c) data, which is remarkable in view of the strongly structured $c = p_0$ and $p_{1,2}$ strength distributions. Fair agreement is still observed for the much lower amount of $E1$ strength in the α_0 channel, even if several fine-structure peaks are at variance.

In the range $14 < \omega < 22$ MeV the total extracted $E2$-$E0$ strength exhausts $(35.5 \pm 2)\%$ of the *electromagnetic* $E2$ EWSR, or $(71 \pm 4)\%$ of the *isoscalar* $E2$ EWSR which is about twice the value of $(34 \pm 6)\%$ deduced from α scattering.[7–9] The $E2$-$E0$ strength in the exclusive *isocalar* $(e,e'\alpha)$ channel shows a distinct resonant behavior (Fig. 3) in qualitative agreement with the isoscalar GMR and GQR structures observed in (α,α')[7–10] and $(\alpha,\alpha'\alpha)$[11] studies also exhibiting a distinct falloff at $E_x \sim 21$ MeV. Considering the possible effects of even weak isospin mixing,[22] we find the absolute strengths extracted from the $(e,e'\alpha)$ and

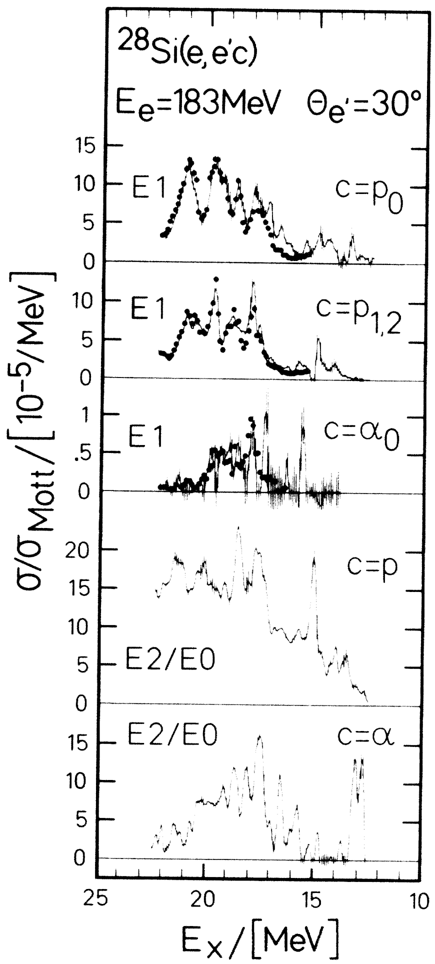

FIG. 3. The deduced $E1$ and $E2$-$E0$ strength distributions in indicated decay channels c. Dots represent for comparison the regularized $E1$ strengths deduced from a $^{28}\text{Si}(\gamma,c)$ study (Ref. 6) with tagged photons.

$(\alpha,\alpha'\alpha)$ studies also at little variance (Table I). In striking contrast to this and different from the $(\alpha,\alpha'p)$ results, the $E2$-$E0$ strength in the *isoscalar* as well as *isovector* $(e,e'p)$ channel (Fig. 3) keeps rather a flat and high level, tending even to increase beyond $E_x = 21$ MeV. Moreover, the $E2$-$E0$ strengths in the p channels show in the electron-induced reaction nearly 3 times the value gained from the $(\alpha,\alpha'p)$ study[11] (Table I). The excess of $E2$-$E0$ strength is thus clearly localized in the p channels $[\Gamma_p/\Gamma_\alpha \sim 2.5$ and 1 in $(e,e'c)$ vs $(\alpha,\alpha'c)]$. Γ_p/Γ_α being ~ 1 for both GMR and GQR,[23] we find convincing evidence for the presence of large isovector $E2$-$E0$ components in the region of the isoscalar GQR and GMR. A similar conclusion was recently suggested from an analysis[24] of π^-/π^+ scattering on ^{118}Sn.

The presence of considerable isovector $E2$-$E0$ strength at much lower excitation energy than expect-

TABLE I. Comparison of the $E2$-$E0$ strengths S_2 in various decay channels c as deduced from the present $(e,e'c)$ study and a previous $(\alpha,\alpha'c)$ experiment (Ref. 11) in the giant resonance region of ^{28}Si. Quoted values of S_2 are given in fractions of the isoscalar $E2$ energy-weighted sum rule.

c	$S_2(e,e'c)$ (%)	$S_2(\alpha,\alpha'c)$ (%)	Ratio
α_0	3.0 ±0.2	3.5 ±0.9	0.9
α_1	14.3 ±0.7	8.9 ±1.9	1.6
All α_i	20 ±1	16 ±3	1.3
p_0	1.5 ±0.8	7.0 ±1.6	2.2
$p_{1,2}$	13.4 ±0.7	6.4 ±1.5	2.1
All p_i	51 ±3	18 ±3	2.8
Total	71 ±4	34 ±6	2.1
Γ_p/Γ_α	2.6	1.1	2.3

ed ($\sim$40 MeV) implies a widely spread $E2$-$E0$ strength distribution and helps to constrain microscopic theories of the decay widths of GR's. Our results are consistent with the previous failure of numerous single-arm scattering studies to identify compact isovector $E2$ strength as discussed, e.g., by Erell *et al.*,[25] and demonstrate the power of the present approach to unravel even very broad multipole excitations in the continuum.

We acknowledge the help of J. R. Calarco in the early stages of the experiment. This work was supported in part by Deutsche Forschungsgemeinschaft (Sonderforschungsbereich 201).

[1]T. W. Donnelly and J. D. Walecka, Annu. Rev. Sci. **25**, 9 (1975).

[2]J. Heisenberg and H. P. Blok, Annu. Rev. Nucl. Part. Sci. **33**, 569 (1983).

[3]J. LeRose *et al.*, Phys. Rev. C **32**, 449 (1985).

[4]J. Ahrens *et al.*, Nucl. Phys. **A251**, 479 (1975).

[5]A. Vessière *et al.*, Nucl. Phys. **A227**, 513 (1974).

[6]R. L. Gulbranson *et al.*, Phys. Rev. C **27**, 470 (1983).

[7]K. T. Knöple *et al.*, Phys. Lett. **64B**, 263 (1977).

[8]D. H. Youngblood *et al.*, Phys. Rev. C **15**, 1644 (1977).

[9]K. van der Borg *et al.*, Phys. Lett. **67B**, 405 (1977).

[10]Y.-W. Lui *et al.*, Phys. Rev. C **31**, 1643 (1985).

[11]K. T. Knöpfle *et al.*, Phys. Rev. Lett. **46**, 1372 (1981).

[12]H. Herminghaus *et al.*, Nucl. Instrum. Methods **138**, 1 (1976).

[13]H. Ehrenberg *et al.*, Nucl. Instrum. Methods **105**, 253 (1972).

[14]W. Kleppinger and J. D. Walecka, Ann. Phys. (N.Y.) **146**, 349 (1983).

[15]Th. Kihm, doctoral thesis, Heidelberg, 1985 (unpublished).

[16]M. Sasso and Y. Torizuka, Phys. Rev. C **15**, 217 (1977).

[17]R. Pitthan *et al.*, Phys. Rev. C **19**, 299 (1979).

[18]M. Goldhaber and E. Teller, Phys. Rev. **74**, 1046 (1948).

[19]L. J. Tassie, Austr. J. Phys. **9**, 407 (1956).

[20]DWBA calculations have been performed with the code HADES [H. G. Andresen *et al.*, International Conference on Nuclear Physics and Electromagnetic Probes, Mainz, 1979 (unpublished), contributed paper No. 8.1] using for the ground-state charge density a three-parameter Fermi distribution with $c_0=3.30$ fm, $a_0=0.545$ fm, and $w_0=-0.18$.

[21]H. Steinwedel and H. Jensen, Z. Naturforsch. **5a**, 413 (1950).

[22]K. T. Knöpfle, in *Nuclear Physics with Electromagnetic Interactions*, edited by H. Arenhövel and D. Drechsel, Lecture Notes in Physics Vol. 108 (Springer-Verlag, New York, 1979).

[23]Y. Toba, U. Garg, Y.-W. Lui, D. H. Youngblood, P. Grabmayr, K. T. Knöpfle, and G. J. Wagner, to be published.

[24]J. L. Ullmann *et al.*, Phys. Rev. Lett. **51**, 1038 (1983).

[25]A. Erell *et al.*, Phys. Rev. Lett. **52**, 2134 (1984).